Adsorption-controlled transition of the electrical properties realized in Hematite (alpha-Fe_2O_3) nanorods ethanol sensing*

Wang Chong(王 翀)[a)†], Wang Fei-Fei(王菲菲)[b)], Fu Xing-Qiu(付星球)[c)], Zhang En-Di(张恩迪)[d)], and Xu Zhi(许 志)[d)]

[a)] *School of Opto-electronic Information Science and Technology, Yantai University, Yantai* 264005, *China*

[b)] *School of Physics, Ludong University, Yantai* 264025, *China*

[c)] *Mathematics and Physics Department, North China Electric Power University, Beijing* 102206, *China*

[d)] *Micro-Nano Technologies Research Center, Hunan University, Changsha* 410082, *China*

(Received 16 October 2010; revised manuscript received 16 December 2010)

Alpha-Fe_2O_3 nanorods are synthesized through a hydrothermal method with no surfactant introduced and ethanol sensors are fabricated from these nanorods. The device can respond to ethanol vapour in a concentration range from 1 to 1500 parts per million and shows both p-type and n-type responding characteristics during the investigation of the ethanol sensing. The sensor displays a p-type characteristic when the ethanol concentration is low and converted into an n-type characteristic as the concentration exceeds a certain value. Such a phenomenon is attributed to the chemisorbed oxygen, which leads to different modifications of the energy band at the surface, namely, depletion layer or inversion layer.

Keywords: adsorption, sensing, depletion, oxygen

PACS: 07.07.Df, 73.63.Bd, 81.07.Bc **DOI:** 10.1088/1674-1056/20/5/050701

1. Introduction

Nanomaterials have potential applications in many fields due to their unique physical and chemical properties.[1−4] Gas sensors are based on the tuning of the electrical properties induced by gas adsorption,[5,6] and they play important roles in fields such as traffic safety, industry production, process control and environment monitoring. Gas sensors realised from oxides particle film,[7] porous film[8] and polymer film[9] have been reported. Recently, great interest has been focused on gas sensors based on quasi one-dimensional nanostructures such as nanowires, nanorods and nanobelts including ZnO, SnO_2, $ZnSnO_3$, CuO/SnO_2,[10−17] and so on. Gas adsorption in certain surroundings evidently modifies the energy band at the surface of nanosized materials due to their large surface-volume-ratio. Such a modification leads to a change of conductivity, which can even induce transition from n-type conductivity to p-type conductivity for materials with a certain band structure.[18−21] The adsorption-controlled conductivity transition makes the device partly free from element impurity, which facilitates applications of these materials in the nanodevices. Nanorods or nanowires of such a characteristic, with less grain boundaries and more convenience in assembly, may have potential applications in electronic intrigue. Alpha-Fe_2O_3 (α-Fe_2O_3) is the most stable iron oxide with easy collection and good resistance to corrosion, which can meet the demands for stability and low cost of nanodevices. Generally, α-Fe_2O_3 is n-type semiconductor in bulk state with a band gap of about 2.1 eV[22] and controlled doping is easy to carry out due to its band structure.[23] In addition, their applications in gas sensing and the adsorption-controlled conductivity are worthy of further research.

In this article, α-Fe_2O_3 nanorods are synthesized through a hydrothermal method. Gas sensors are fabricated from these Fe_2O_3 nanorods and their responses

*Project supported by the National Basic Research Program of China (Grant No. 2007CB310500), the National Natural Science Foundation of China (Grant No. 90606009), the Funds for Doctor of Yantai University, China (Grant No. WL08B8), the Funds for Doctor of Ludong University, China (Grant No. LY20082802), and the Natural Science Foundation of Hunan Province, China (Grant No. 10JJ1011).

†Corresponding author. E-mail: fyfyforever@163.com

© 2011 Chinese Physical Society and IOP Publishing Ltd

to ethanol are investigated. As the ethanol concentration varies from 1 to 1500 parts per million (ppm), the electrical properties of the nanorods transits from p-type sensing characteristics to n-type characteristics. Below the transiting point, the sensor resistance turns bigger when exposed to ethanol vapour. Above the transiting point, the sensor resistance decreases when ethanol concentration increases. Such a phenomenon is attributed to the modification to the band structure of α-Fe_2O_3 nanorods induced by oxygen adsorption.

2. Experimental details

The α-Fe_2O_3 nanorods were synthesized through an improved hydrothermal method free from surfactant. 1–10 g iron chloride ($FeCl_3{\cdot}6H_2O$) of analytical grade was dissolved into 40 ml distilled water. Dark yellow homogeneous solution was obtained in 30 min stirring. Then the solution was transferred into Teflon-lined stainless steel autoclave with a volume capacity of 50 ml. After being kept in the oven at 120 °C for 12 h, the autoclave was cooled down to room temperature naturally. During the reaction, $[Fe(H_2O)_6]^{3+}$ was hydrolyzed to form β-FeOOH precursor and then the precursor changed into α-Fe_2O_3 via the dissolution/reprecipitation mechanism.[24,25] The yellow collection was washed with distilled water and absolute ethanol for several times to remove the remains of Fe^{3+} and Cl^- ions. Then morphology and crystalline structure of the as-prepared sample were analysed by scanning electron microscope (SEM: JEOL-JSM-4200F) and transmission electron microscope (TEM: Tecnai F20) and x-ray powder diffraction (XRD: D/max 2550 V, Cu Kα radiation) respectively.

3. Results and discussion

Crystal structures and phases of the products were determined from the XRD pattern. Figure 1 shows the XRD pattern of the as-prepared product. All the diffraction peaks are indexed to the α-Fe_2O_3 with lattice constants of $a = 5.032$ Å (1 Å=0.1 nm) and $c = 13.74$ Å (JCPDS: 87-1166).

The morphology of the as-prepared sample was revealed by the SEM image as shown in Fig. 2(a). The nanorods are about 160 nm in diameter and 2 μm in length. Figure 2(b) shows the TEM image of the nanorods for detailed information about their structure. The spacing marked in the image is measured to be 0.367 nm, which matches the interplanner space of the crystal planes with orientation index [012]. The result demonstrates that the nanorods grow along the direction parallel with the crystal plane (012).

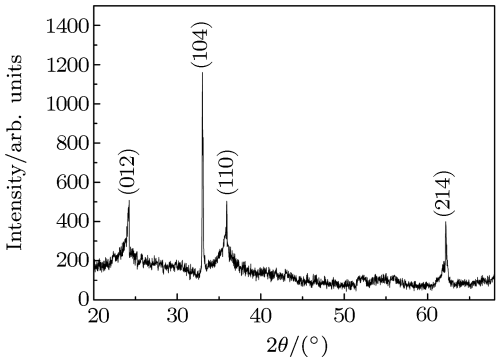


Fig. 1. XRD pattern of as-prepared sample.

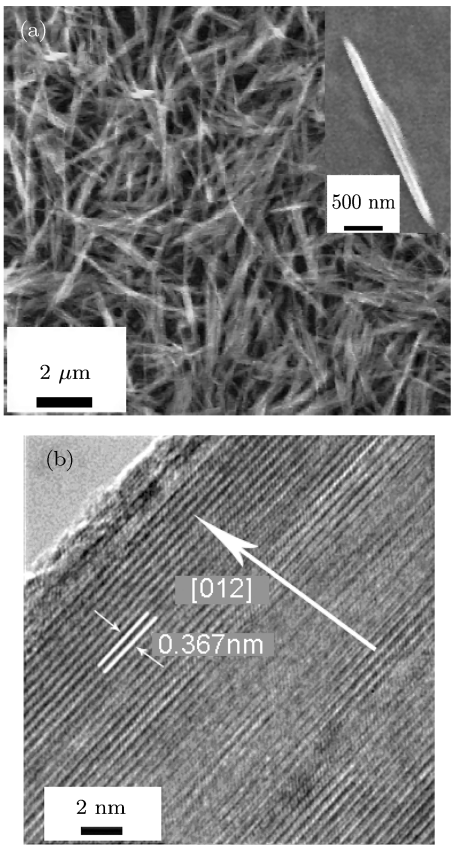


Fig. 2. (a) SEM image of the Fe_2O_3 nanorods and the inset showing the image of a single nanorods; (b) high resolution TEM image of the nanorod.

The gas sensor was fabricated by dispersing the as-prepared α-Fe_2O_3 nanorods between two gold electrodes as described in Ref. [26]. Then the sensor was annealed in the air at 400 °C for 48 h for requirement of stability. The circuit for measurement was as indicated in Ref. [27]. The circuit for the measurement

had a heating loop which offered a local operating temperature of 300 °C to accelerate the surface reacting rate. And we selected a reference resistance of 4700 kΩ to match that of the sensor. Because the sensor was in series with the reference resistance, so the transition of sensor resistance could be reflected by the change of the voltage crossing the reference resistance.

The ethanol sensing characteristic of the device at low concentration was shown in Fig. 3(a). The investigation was carried out when the ethanol concentration varied from 1 to 50 ppm. As exposed to ethanol vapour, the resistance of the sensor became lower than that in the air. With the increase of ethanol concentration, the sensor resistance first increased and then decreased. Then the response to ethanol vapour of relatively high concentration was investigated and the sensing characteristic was exhibited in Fig. 3(b). The concentration of ethanol vapour ranged from 100 to 1500 ppm in the investigation. The sensor resistance decreased as the ethanol concentration increased, which was contrary to the scenario revealed at low concentration. Change of the sensor resistance with ethanol concentration can be deduced from the change of the voltage. The sensor showed different sensing characteristics at different ethanol concentrations which led to different oxygen chemisorptions and physisorptions at the surface.

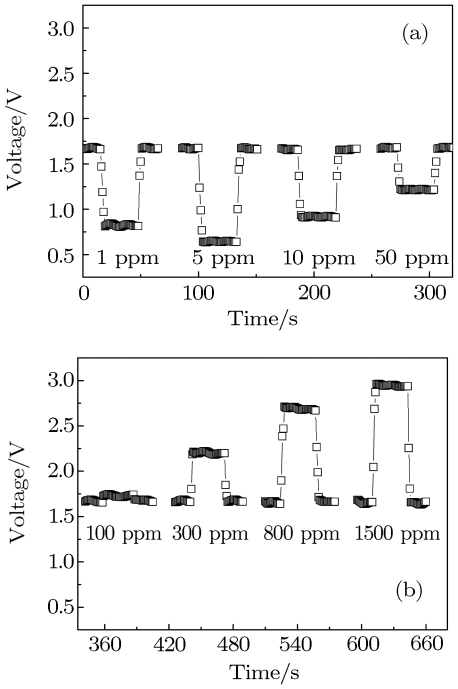


Fig. 3. Ethanol sensing characteristic of the Fe_2O_3 nanorods at concentrations (a) from 1 to 50 ppm and (b) from 100 to 1500 ppm.

Usually, gas molecules adsorbed on the nanorods surface will influence the electrical properties by affecting the concentration of carriers as well as the height of contacting barriers. For n-type semiconductors, the majority of carriers are electrons. As they are exposed to the air, the chemisorbed oxygen molecules will trap electrons from the nanorods, which leads to the formation of depletion layers at the surface of the nanorods.[10] The built-in electrical field induced by the transferred charges acts as barriers for electrons transport between the nanorods according to the grain boundary model.[13,28] When the n-type semiconductor is exposed to reductive gas, the adsorbed oxygen is eliminated from the surface and the trapped electrons are released back to the nanorods. So, generally, the sensor resistance based on an n-type semiconductor decreases as the sensor is moved from air to ethanol. While in our experiments, sensor based on α-Fe_2O_3, shows p-type sensing characteristic with exposure to ethanol of low concentration and n-type characteristic in ethanol vapour of high concentration. Such a phenomenon results from the modification to the energy band at the surface induced by the oxygen adsorption. The densities of carriers crossing the space charge layer are determined by the following functions:

$$\begin{aligned} n_{\rm s} &= N_{\rm c}\exp\{-(E_{\rm c}+eV_{\rm s}-E_{\rm f})/kT\} \\ &= N_{\rm c}\exp\{-(E_{\rm i}+E_{\rm g}/2+eV_{\rm s}-E_{\rm f})/kT\}, \quad (1) \end{aligned}$$

and

$$\begin{aligned} p_{\rm s} &= N_{\rm v}\exp\{-(E_{\rm f}-E_{\rm v}-eV_{\rm s})/kT\} \\ &= N_{\rm v}\exp\{-(E_{\rm f}-E_{\rm i}+E_{\rm g}/2-eV_{\rm s})/kT\}. \quad (2) \end{aligned}$$

Here, $eV_{\rm s}$ is the variation of the potential in the space charge field; $V_{\rm s}$ can be expressed as $V_{\rm s} = eN_{\rm s}^2/(2\varepsilon_0\varepsilon_{\rm r}D^+)$ according to one-dimensional Poisson equation,[5] where D^+ is the density of the singly charged acceptors and $N_{\rm s}$ is equal to the multiple of D^+ and the Deybe length or the depth of the space charge layer; $E_{\rm i}+eV_{\rm s}$ is the intrinsic Fermi level at the surface. The conductivity characteristic of the surface charge layer is determined by the relative position between the intrinsic energy level and the Fermi level. With a little chemisorbed oxygen, the height of surface potential is relatively low, which keeps $E_{\rm i}+eV_{\rm s}$ below the Fermi level. The ratio between major and minor carriers can be described as $n_{\rm s}/p_{\rm s} = (N_{\rm c}/N_{\rm v})\exp(2\Delta/kT)$. Considering $\Delta = E_{\rm f}-E_{\rm i}-eV_{\rm s} > 0$, such a band structure still contributes to the n-type conducting characteristic. With much oxygen chemisorbed, the intrinsic energy level at the surface exceeds the Fermi level, which

leads to the formation of surface inversion layer. Correspondingly, the holes in the space charge layer will play a major role with the ratio of n_s/p_s decreasing exponentially when $\Delta < 0$. And additionally, the high surface potential acts as barriers only for electrons, so the medium will represent p-type conducting characteristics. During our experiments, when the sensor based on Fe_2O_3 was exposed to ethanol of high concentration, only a little chemisorbed oxygen remained at the surface. So n-type sensing is investigated due to the mechanism of depletion layer.[10,13,28] When the sensor is exposed to ethanol gas with low concentration, most adsorbed oxygen atoms remain at the surface. The intrinsic energy level keeps higher than the Fermi level at the surface, so the sensor resistance increases with the ethanol concentration decreasing, which matches the p-type conductivity characteristic. Such a phenomenon cannot be investigated in bulk α-Fe_2O_3. Transition like this is related to the size of the material. The Fermi level is related only to the state density of electrons and can be expressed as $E_f = (\hbar^2/2m)(3\pi^2 n)^{2/3}$, where n is the state density of electrons. Oxygen adsorption will reduce the electron density by the density of acceptors D^+.[5] So the Fermi level changes more or less during the ethanol sensing. For bulk Fe_2O_3, n being much greater than D^+, eV_s is so small compared with E_f that the tuning effect of oxygen adsorption can be ignored in the electron transportation. Then the n-type conductivity keeps unchanged in ambient atmosphere. While for nanosized Fe_2O_3, depth of the depletion layer is almost on the same scale as the diameter of the nanorods due to their large surface-volume-ratio and small diameter, which means lower Fermi level and bigger eV_s. Then the sample will show p-type conducting characteristics when $n_s/p_s = (N_c/N_v)\exp(2\Delta/kT)$ decreases to a certain degree. The corresponding bands with different oxygen adsorptions are schematically indicated in Fig. 4. The competition between the vacancy conductivity and the electron conductivity leads to the transition at about 10 ppm.

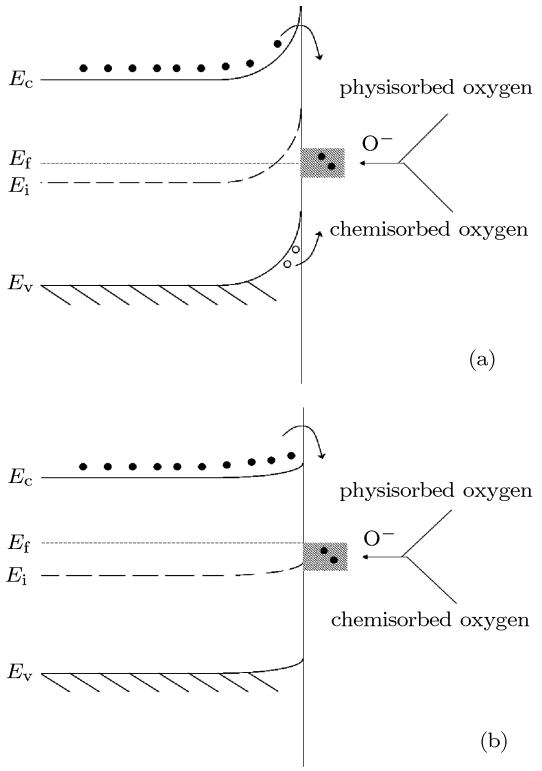


Fig. 4. Schematic diagram of bands with different oxygen adsorptions: (a) the formation of inversion layer (p-type, low ethanol concentration), (b) the formation of depletion layer (n-type, high ethanol concentration).

4. Conclusion

α-Fe_2O_3 nanorods are synthesized through a hydrothermal method free from surfactant and ethanol sensors are fabricated from these nanorods. The ethanol sensing characteristics are investigated and a reversible transition of the conductivity between n-type characteristic and p-type characteristic is found. The sensing mechanism is analysed in terms of the depletion model and grain boundary model. The transition is explained by the transition from depletion layer to inversion layer due to the oxygen-controlled surface potential as well as the small size of the nanorods. Such a transiting characteristic facilitates the application of α-Fe_2O_3 nanorods in junction-like devices and detecting devices.

References

[1] Yang Y R, Yan X H, Guo Z H and Deng Y X 2008 *Chin. Phys.* B **17** 3433

[2] Ma W G, Wang H D, Zhang X and Takahashi Koji 2009 *Chin. Phys.* B **18** 2035

[3] Liu C M, Fang L M and Zu X T 2009 *Acta Phys. Sin.* **58** 936 (in Chinese)

[4] Huang J Z, Li S S and Feng X P 2010 *Acta Phys. Sin.* **59** 5839 (in Chinese)

[5] Batzill M and Diebold U 2005 *Prog. Surf. Sci.* **79** 47

[6] Collins P G, Bradley K, Ishigami M and Zettl A 2000 *Science* **287** 10

[7] Ogawa H, Nishikawa M and Abe A 1982 *J. Appl. Phys.* **53** 4448

[8] Lin H M, Hsu C M, Yang H Y, Lee P Y and Yang C C 1994 *Sens. Actua.* B **22** 63

[9] Zamborini F P, Leopold M C, Hicks J F, Kulesza P J, Malik M A and Murray R W 2002 *J. Am. Chem. Soc.* **124** 8958

[10] Wan Q, Li Q H, Chen Y J, Wang T H, He X L, Li J P and Lin C L 2004 *Appl. Phys. Lett.* **84** 3654

[11] Li Q H, Liang Y X, Wan Q and Wang T H 2004 *Appl. Phys. Lett.* **85** 6389

[12] Ying Z, Wan Q, Song Z T and Feng S L 2004 *Nanotechnology* **15** 1682

[13] Feng P, Wan Q and Wang T H 2005 *Appl. Phys. Lett.* **87** 213111

[14] Scott R W J, Yang S M, Chabanis G, Coombs N, Williams D E and Ozin G A 2001 *Adv. Mater.* **13** 1468

[15] Chen Y J, Xue X Y, Wang Y G and Wang T H 2005 *Appl. Phys. Lett.* **87** 233503

[16] Xue X Y, Chen Y J, Wang Y G and Wang T H 2005 *Appl. Phys. Lett.* **86** 233101

[17] Kong X and Li Y 2005 *Sens. Actua.* B **105** 449

[18] Bielanski A, Deren J and Haber J 1957 *Nature* **179** 668

[19] Bârsan N, Grigorovici R, Ionescu R, Motronea M and Vancu A 1989 *Thin Solid Films* **171** 53

[20] Savage N, Chwieroth B, Ginwalla A, Patton B R, Akbar A and Dutta P K 2001 *Sens. Actua.* B **79** 17

[21] Korotcenkov G, Brinzari V, Golovanov V, Cerneavschi A, Matolin V and Todd A 2004 *Appl. Surf. Sci.* **227** 122

[22] Mohanty S and Ghose J 1992 *J. Phys. Chem. Sol.* **53** 81

[23] Fan Z Y, Wen X G, Yang S H and Lu J G 2005 *Appl. Phys. Lett.* **87** 013113

[24] Musić S, Vértes A, Simmons G W, Czakló-nangy I and Leiodheioser H 1982 *J. Coll. Interf. Sci.* **85** 256

[25] Gotić M, Popović S, Ljubešić N and Musić S 1994 *J. Mater. Sci.* **29** 2474

[26] Wang C, Fu X Q, Xue X Y, Wang Y G and Wang T H 2007 *Nanotechnology* **18** 145506

[27] Gao T and Wang T H 2005 *Appl. Phys.* A **80** 1451

[28] Kiss G, Pintér Z, Perczel I V, Sassi Z and Réti F 2001 *Thin Solid Films* **391** 216